

Assessment of Tumor Energy and Oxygenation Status by Bioluminescence, Nuclear Magnetic Resonance Spectroscopy, and Cryospectrophotometry¹

W. Mueller-Klieser,² C. Schaefer, S. Walenta, E. K. Rofstad, B. M. Fenton, and R. M. Sutherland

Institute of Physiology and Pathophysiology, University of Mainz, Saarstrasse 21, D-6500 Mainz, Federal Republic of Germany [W. M.-K., C. S., S. W.]; Institute for Cancer Research and The Norwegian Cancer Society, The Norwegian Radium Hospital, Montebello, 0310 Oslo 3, Norway [E. K. R.]; Experimental Therapeutics Division and Departments of Radiation Oncology and Biophysics, University of Rochester Cancer Center, Rochester, New York 14642 [B. M. F., R. M. S.]; and SRI International, Life Sciences Division, Menlo Park, California 94025 [R. M. S.]

ABSTRACT

The energy and oxygenation status of tumors from two murine sarcoma lines (KHT, RIF-1) and two human ovarian carcinoma xenograft lines (MLS, OWI) were assessed using three independent techniques. Tumor energy metabolism was investigated *in vivo* by ³¹P nuclear magnetic resonance spectroscopy. After nuclear magnetic resonance measurements, tumors were frozen in liquid nitrogen to determine the tissue ATP concentration by imaging bioluminescence and to register the intracapillary oxyhemoglobin (HbO₂) saturation using the cryospectrophotometric method.

There was a positive correlation between the nucleoside triphosphate β/total resonance ratio or a negative correlation between the P_i/total resonance ratio and the model ATP concentration obtained by bioluminescence, respectively. This was true for small tumors with no extended necrosis irrespective of tumor type. Moreover, a positive correlation was obtained between the HbO₂ saturations and the ATP concentration measured with bioluminescence. The results demonstrate the potential of combined studies using noninvasive, integrating methods and high-resolution imaging techniques for characterizing the metabolic milieu in tumors.

INTRODUCTION

The significance of the metabolic milieu in relation to tumor growth and susceptibility to treatment has been well documented by numerous investigations (for reviews, see Refs. 1 and 2). Among the various parameters determining the biological behavior of tumors, the tissue oxygenation and the energy status of tumor cells seem to play a crucial role (3, 4). These critical determinants of the cellular environment in tumors have been assessed by a number of invasive techniques, *e.g.*, by microelectrodes (5), by cryospectrophotometry (6-8), and by enzymatic assays (9). More recently, noninvasive methods have been used for characterizing tumor metabolism, such as NMR³ spectroscopy and positron emission tomography (4, 10-13).

Although advantageous for clinical application, noninvasive techniques lack high spatial resolution and, at least in parts, are difficult to calibrate in absolute terms. The combination of these methods with imaging bioluminescence (14, 15) may be useful for a better evaluation of the biological and clinical relevance of data obtained from the noninvasive techniques mentioned.

The present study was performed to compare data on tumor energy and oxygenation status assessed by ³¹P NMR spectroscopy, bioluminescence, and cryospectrophotometry in the same

tumors. Thereby, average values were evaluated for the comparison to be made.

MATERIALS AND METHODS

Four tumor lines, 2 murine sarcomas (KHT and RIF-1), and 2 human ovarian carcinoma xenografts (MLS and OWI), were used in the present work. The KHT (16) and RIF-1 (17) tumors were initiated by inoculating 2×10^5 cells *s.c.* into the flank of 8-10-week-old female C3H/HeJ mice (The Jackson Laboratory, Bar Harbor, ME). The RIF-1 tumor line was maintained alternately *in vivo* and *in vitro* according to the protocol established by Twentyman *et al.* (17), in order to minimize genetic drift and development of antigenicity. The MLS and OWI tumors were initiated by transplanting tissue fragments, approximately $2 \times 2 \times 2$ mm, *s.c.* into the flank of 8-10-week-old female BALB/c athymic mice (Sciences, Inc., St. Petersburg, FL) kept in a humidified, aseptic environment (8). Tumor volumes were measured with calipers. Two perpendicular diameters (length and width) were recorded and tumor volumes were calculated as

$$V = \frac{1}{2} ab^2$$

where *a* and *b* are the longest and the shortest diameter, respectively.

³¹P spectra were obtained using solenoidal coils and a General Electric 2T CSI spectrometer with a working magnet bore of 22 cm operating at 34.635 MHz for phosphorus as described previously (18). The acquisition parameters were: 4-μs pulse length; 1000-Hz spectrum sweep width; 4000 data points/free induction decay; 1000-ms repetition time. The number of acquisitions per spectrum was always 1024 to ensure a good signal:noise ratio. The free induction decays were subjected to an exponential line broadening of 10 Hz prior to Fourier transformation. Resonance areas were calculated from phased, resolution-enhanced, baseline-corrected spectra by applying a curve-fitting procedure based on the least squares minimization technique and assumed Lorentzian peak shapes. Intracapillary HbO₂ saturations were measured by reflection cryospectrophotometry using a modification of the four wavelength method of Gayeski (19), as described by Rofstad *et al.* (8). Measuring wavelengths of 557 and 578 nm and "isosbestic" wavelengths of 565 and 584 nm were applied in the present work. The HbO₂ saturation status of the tumors was fixed by rapid freezing *in vivo* at liquid nitrogen temperature. Two to five representative surfaces were prepared from each tumor and vessels with a diameter larger than 12 μm were randomly selected from the surfaces for measurement of HbO₂ saturations. A total of 100 vessels were analyzed for each tumor.

Metabolic imaging with bioluminescence has been described by Mueller-Klieser *et al.* (14, 15). The technique makes it possible to measure local concentrations of metabolites, such as glucose, lactate, and ATP, by linking the substance of interest to the luminescence of luciferase through appropriate enzymes. The spatial distribution of ATP was assessed here in cryostat sections of rapidly frozen tissue biopsies. For imaging, each cryostat section was kept frozen and was covered with a cryostat section of the frozen enzyme cocktail. The enzyme reaction and subsequent photon emission was then started by thawing the sections; the light intensity was evaluated by film exposure or by an imaging photon counting system (Hamamatsu Photonics Europa GmbH, Herrsching, Federal Republic of Germany).

Imaging bioluminescence was used to register the distributions of ATP concentration calibrated in absolute terms. The concentration of ATP was obtained in mM with respect to tissue volume by comparing

Received 7/20/89; revised 11/18/89.

The costs of publication of this article were defrayed in part by the payment of page charges. This article must therefore be hereby marked *advertisement* in accordance with 18 U.S.C. Section 1734 solely to indicate this fact.

¹ This work was supported by the Deutsche Forschungsgemeinschaft (Mu 576/2-3), by the Bundesministerium für Forschung und Technologie (01ZO8801/0), and by grants from The National Cancer Institute (CA-20329 and CA-11198) and The Norwegian Cancer Society.

² To whom requests for reprints should be addressed, at Institute of Physiology and Pathophysiology, University of Mainz, Saarstrasse 21, D-6500 Mainz, Federal Republic of Germany.

³ The abbreviations used are: NMR, nuclear magnetic resonance; NTP, nucleoside triphosphate.

the bioluminescent intensity of the actual tissue section with that of standard sections. Metabolically inactivated tissue homogenates containing different ATP concentrations served as standards. The ATP concentrations in the homogenates were determined by high-pressure liquid chromatography. Multiple determinations of ATP in standards with bioluminescence demonstrated a precision of $\pm 5\%$ (SD) with respect to the coefficient of variation within a physiologically relevant concentration range. Differences in ATP values measured with bioluminescence and with high-pressure liquid chromatography in the same samples were usually within the accuracy of the two techniques. Tissue sections with a low quality in their histological structure often gave rise to inconsistent data and were therefore excluded from measurement.

During ^{31}P NMR spectroscopy and freezing of the tumors for HbO₂ cryospectrophotometry and ATP bioluminescence imaging, the mice were anesthetized with sodium pentobarbital, 0.07 mg/g body weight for the C3H/HeJ mice and 0.09 mg/g body weight for the BALB/c athymic mice, and were kept at normal body core temperature (37–38°C) by using a heating pad with circulating water. When the body core temperature was controlled, the anesthesia itself was found to have insignificant effects, if any at all, on the ^{31}P NMR spectral parameters (20).

For statistical evaluation, the frequency distributions of the measuring values were registered.

RESULTS

Ten tumors in the volume range of 150–600 mm³ (3 RIF-1, 2 KHT, 3 MLS, and 2 OWI) were studied in the present work. Tumors of different lines were chosen in an attempt to cover a broad range of values for ATP concentrations, ^{31}P NMR resonance ratios, and HbO₂ saturations. Fig. 1 shows ATP bioluminescence frequency distributions for 2 tumors, *i.e.*, the tumors presenting the lowest and the highest ATP concentrations.

The ^{31}P NMR spectra were qualitatively similar for all four tumor lines and showed seven clear, major peaks corresponding to phosphomonoesters, P_i, phosphodiesteres, phosphocreatine, and nucleoside triphosphates (NTP_γ, NTP_α, and NTP_β). Fig. 2 shows the ^{31}P NMR spectra for the same 2 tumors for which ATP data are presented in Fig. 1. The tumor with the lowest ATP concentrations showed a lower NTP_β/total resonance ratio than the tumor presenting the highest ATP concentrations.

Frequency distributions for intracapillary HbO₂ saturation for the same 2 tumors are presented in Fig. 3. The majority of the vessels showed HbO₂ saturations below 10%, but values covering the whole range up to above 90% were measured. Intracapillary HbO₂ saturations below about 30% will reflect hypoxic areas in most tumors in mice which can be concluded from model calculations (8). These calculations are based on the assumption that the lowest HbO₂ saturations measured are those at venous ends of tumor microvessels. Using experimental HbO₂ dissociation curves, intercapillary distances, and O₂ consumption rates and diffusivities, it is possible to calculate for the lowest O₂ tension that may occur in the intercapillary region. These O₂ tensions are far above what can be considered radiobiologically hypoxic, if HbO₂ saturations are >30%. The fraction of vessels with HbO₂ saturation above 30% was therefore used as a parameter for the tumor oxygenation status in the present work. Fig. 3 shows that the tumor with the lower ATP concentrations and the lower NTP_β/total resonance ratio also had the lower HbO₂ saturation status and *vice versa*.

In a statistical comparison of data obtained by bioluminescence, NMR, and cryospectrophotometry, the ATP value which occurred most frequently in bioluminescent measurements, *i.e.*, the modal ATP value, showed the closest correlation with ATP-related data assessed by the 2 other techniques.

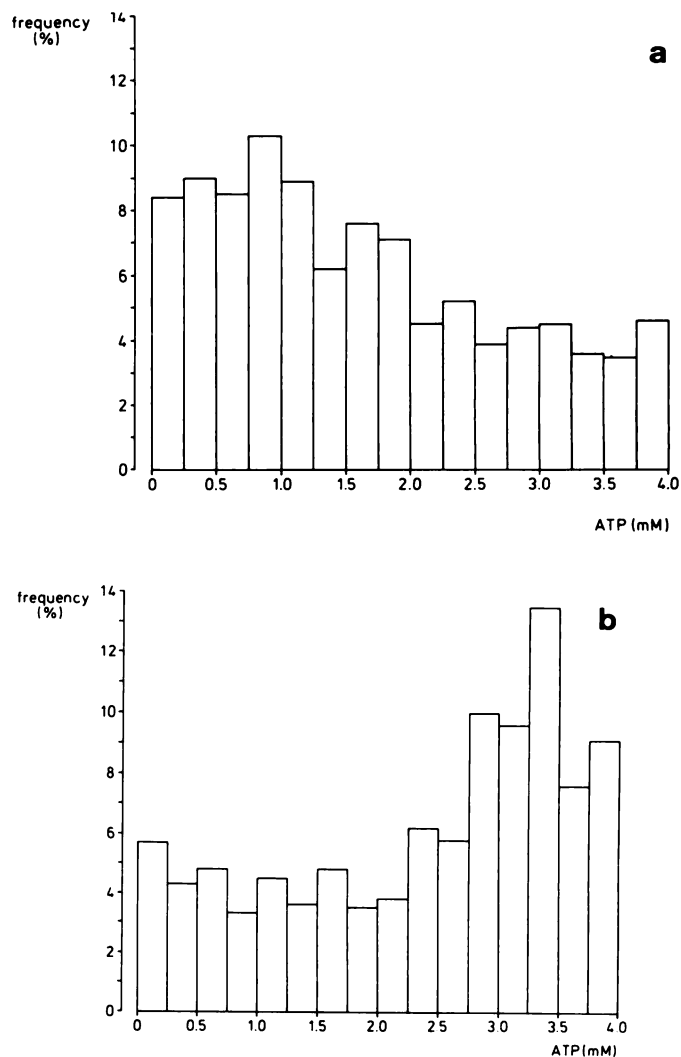


Fig. 1. Frequency distribution of ATP concentration values measured by imaging bioluminescence. *a*, tumor with the lowest modal ATP concentration measured (RIF-1/10; volume, 587 mm³); *b*, tumor with the highest modal ATP concentration measured (MLS/9; volume, 208 mm³).

The modal ATP values obtained from bioluminescence were positively correlated with the NTP_β/total resonance ratio in NMR, as demonstrated in Fig. 4. Correspondingly, an inverse relationship was found between ATP concentrations from bioluminescence measurements and the P_i/total resonance ratio in NMR which is shown in Fig. 5. A positive correlation was obtained in the tumors investigated between ATP concentrations determined by bioluminescence and tumor HbO₂ saturations (Fig. 6). Statistically significant correlations similar to those in Figs. 4–6 were not found when tumors larger than 600 mm³ were analyzed. Finally, modal ATP concentrations measured with bioluminescence decreased with increasing tumor volume, as indicated in Fig. 7.

The data show that there are linear correlations between NMR signals related to the content of energy-rich phosphates in small tumors and the ATP concentrations measured in absolute terms with bioluminescence. Furthermore, the latter parameter is correlated with data on tumor tissue oxygenation assessed by cryospectrophotometry with ATP concentrations being high in relatively well oxygenated tumors and *vice versa*.

DISCUSSION

The present study includes experimental data from 3 independent methods for characterizing the oxygenation and energy

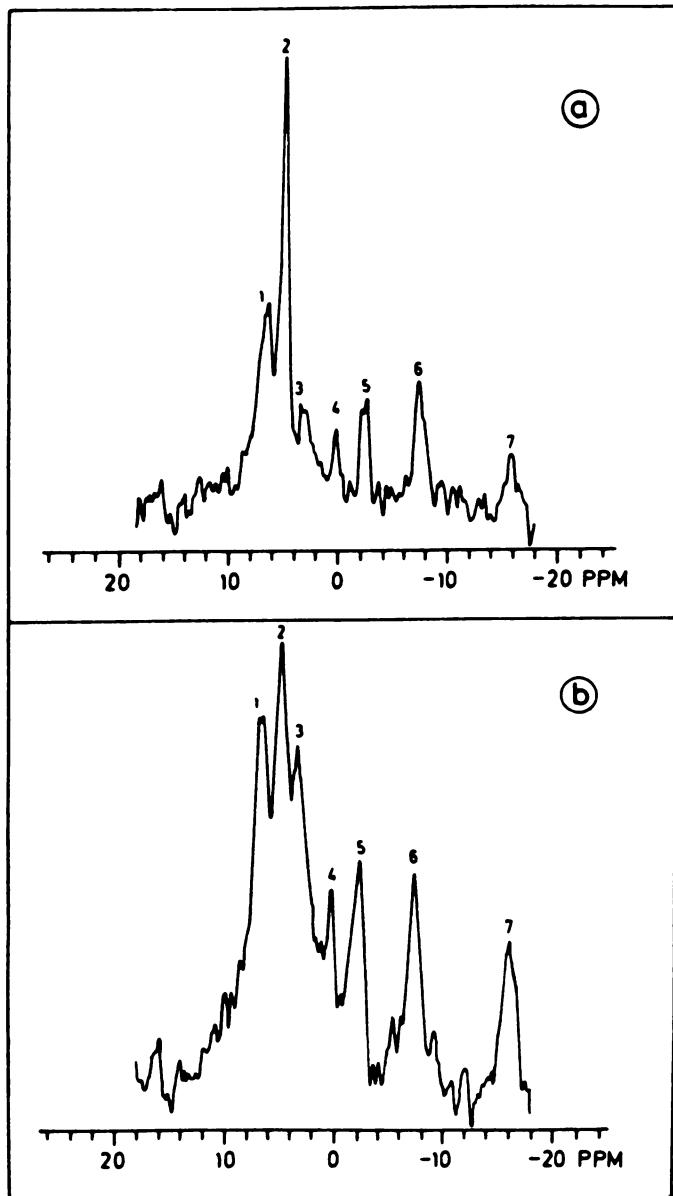


Fig. 2. ^{31}P NMR spectra for (a) a RIF-1/10 tumor (volume, 587 mm^3) and (b) a MLS/9 tumor (volume, 208 mm^3) differing considerably in energy status. The resonance assignment is: Peak 1, phosphomonoesters; Peak 2, P_i ; Peak 3, phosphodiester; Peak 4, phosphocreatine; Peaks 5, 6, and 7, $\text{NTP}\gamma$, $\text{NTP}\alpha$, and $\text{NTP}\beta$, respectively.

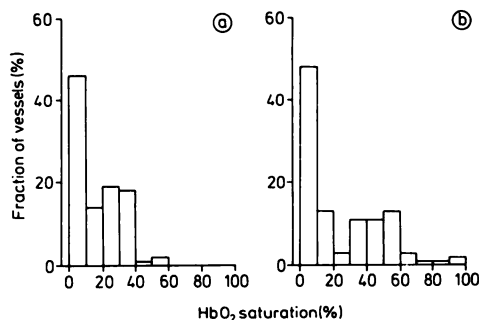


Fig. 3. Frequency distributions for intracapillary HbO_2 saturation for (a) a RIF-1/10 tumor (volume, 587 mm^3) and (b) a MLS/9 tumor (volume, 208 mm^3) differing considerably in oxygenation status. A few vessels gave negative HbO_2 saturation readings slightly below zero due to the random uncertainty in the measurements, and these vessels are included in the first column of the frequency distributions. A total of 100 vessels were analyzed for each tumor.

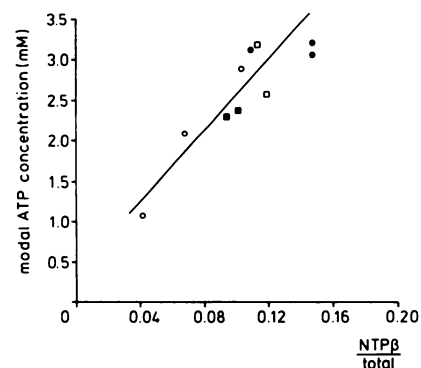


Fig. 4. Modal ATP concentration measured with imaging bioluminescence in various rodent tumors and human tumor xenografts plotted against $\text{NTP}\beta$ magnetic resonance intensity in the same tumors (○, RIF-1/10; ●, MLS/9; □, OWI; ■, KHT; $n = 10$; $y = 22.27x + 0.35$; $r = 0.908$; $2\alpha < 0.001$).

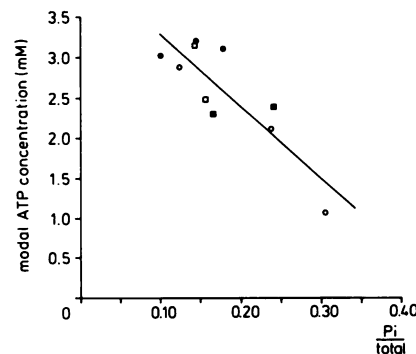


Fig. 5. Modal ATP concentration determined with imaging bioluminescence in the tumors shown in Fig. 3 plotted against P_i magnetic resonance intensity (symbols as shown in Fig. 4; $n = 10$; $y = -8.92x + 4.18$; $r = -0.854$; $2\alpha < 0.01$).

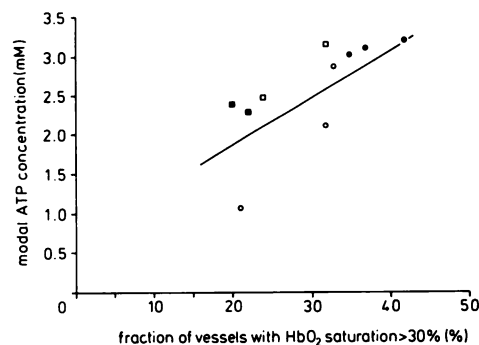


Fig. 6. Modal ATP concentration measured with imaging bioluminescence in the tumors shown in Fig. 3 plotted against fraction of vessels with oxyhemoglobin saturations larger than 30% (symbols as shown in Fig. 4; $n = 10$; $y = 0.06x + 0.67$; $r = 0.728$; $2\alpha < 0.05$).

status of tumors. The experiments were conducted in 2 different laboratories by various investigators. The measurements that were made in 4 different tumor lines required the transportation of cryobiopsies over a long distance. Taking into account the hazards inherent to such a study, the correlations among the measuring values of the different techniques must be considered a mutual validation of the methods applied. Both NMR spectroscopy and cryospectrophotometry provide data that are averaged over the entire tumor. In contrast, the bioluminescent technique yields information on the spatial distribution of metabolites. Consequently, the ATP concentrations obtained by the latter method had to be averaged before they could be related to the data measured with the integrating techniques.

During the evaluation of the measuring values, it became

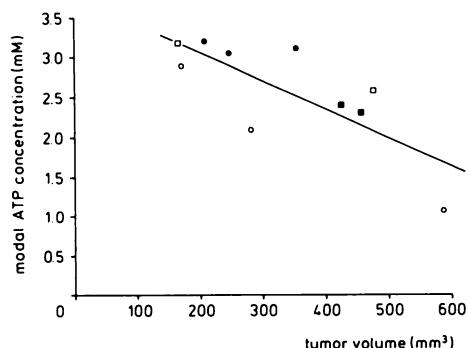


Fig. 7. Modal ATP concentration measured with imaging bioluminescence as a function of tumor volume (symbols as shown in Fig. 4; $n = 10$; $y = 0.0036x + 3.79$; $r = 0.787$; $2\alpha < 0.01$).

obvious that the method of averaging can be crucial for the comparison to be made. Only a weak correlation was found between NMR data and ATP measured with bioluminescence, if mean or median values rather than the mode were considered. A possible explanation for this may be that there is a smearing of the true concentration distribution at the edges of the tissue sections during bioluminescent measurements (14). This artifact is mainly caused by washing out the substance of interest from the section into the surrounding embedding medium. As a consequence, a shallow decline rather than a step function in the photon intensity is obtained at the edge of most of the sections leading to a falsely increased incidence of low intensity measurements. Assuming that the true frequency distribution of measured values would have a Gaussian shape, the actually registered distribution of ATP concentration may then represent a logarithmic normal distribution with asymmetry. Several statistical parameters, such as the mean or the median, will be affected by such a change, whereas the mode of the distribution remains constant.

The region of data sampling was another critical parameter in the present study. Keeping in mind that tumor tissue is often extremely heterogeneous in blood flow and metabolic milieu (5, 7), a close interrelationship between NMR signals integrated over the entire tumor volume and bioluminescence data collected from biopsies cannot be anticipated. Values assessed with these two techniques were not correlated in large tumors with extended necrosis. Presumably, this was mainly due to different amounts of necrosis within the volume of interest which is likely to affect the concentration of energy-rich phosphates. A lower biopsy:tumor size ratio may also contribute to the discrepancies found in large tumors, since the biopsy may be less representative for the entire tumor under such conditions. On the other hand, ATP was determined by the bioluminescence technique in 3–10 cryosections per biopsy arbitrarily distributed over the biopsy volume, which was true for all tumors.

Taking into account these restrictions, the present study demonstrates the potential of combining noninvasive, integrating techniques, such as NMR with cryospectrophotometry and high-resolution imaging techniques, e.g., bioluminescence. The question of number, location, and size of biopsies can be investigated systematically. The biological and clinical significance of averaged *versus* spatially resolved signals can be evaluated. Finally, such a combined study makes it possible to compare the potential of relative measurements of metabolites with that of determining absolute concentration values.

The results obtained confirm earlier measurements on the same tumor types (18) showing a positive correlation between tumor oxygenation and energy status. Corresponding correla-

tions between tissue O_2 tensions and ^{31}P NMR signals were found in a murine fibrosarcoma by Vaupel *et al.* (21). The correlation between tumor oxygenation and ATP content may be quantitatively different in different tumor types which contributes to the scatter in the data obtained. This may be indicated by the circles in Fig. 6 representing means of measuring values in 3 RIF-1 tumors. A regression through these data points may lead to a steeper slope compared to the overall correlation.

A decrease of the tumor ATP content measured with bioluminescence with increasing tumor volume was registered which was true for different tumors of human and rodent origin. Although this correlation was statistically significant, it is obvious that the relationship between tumor size and ATP content is valid only within a certain size range and that this range may be different for different tumor types. This is supported by the finding that the $NTP\beta$ signal in NMR was not correlated with tumor volume in a previous series of experiments with OWI tumors of similar sizes (18). A causative relationship between the two parameters of tumor metabolism cannot be derived from the data obtained; the tissue content of both ATP and oxygen may change by changing either the delivery or the consumption rates, respectively. However, the fact that the uptake rates for oxygen and nutrients of many tumors are determined by the blood supply (3) is strongly suggestive that the energy status of tumors may be dependent on the oxygen supply to tumor tissue.

REFERENCES

- Vaupel, P., and Kallinowski, F. Physiological effects of hyperthermia. *Recent Results Cancer Res.*, **104**: 71–109, 1987.
- Moulder, J. E., and Rockwell, S. Tumor hypoxia: its impact on cancer therapy. *Cancer Metastasis Rev.*, **5**: 313–341, 1987.
- Vaupel, P., Fortmeyer, H. P., Runkel, S., and Kallinowski, F. Blood flow, oxygen consumption and tissue oxygenation of human breast cancer xenografts in nude rats. *Cancer Res.*, **47**: 3496–3503, 1987.
- Okunieff, P., Kallinowski, F., Vaupel, P., and Neuringer, L. J. Effects of hydralazine-induced vasodilation on the energy metabolism of murine tumors studied by *in vivo* P31-nuclear magnetic resonance spectroscopy. *J. Natl. Cancer Inst.*, **80**: 745–750, 1988.
- Vaupel, P., Frinak, S., and Bicher, H. I. Heterogeneous oxygen partial pressure and pH distribution in C3H mouse mammary adenocarcinoma. *Cancer Res.*, **41**: 2008–2013, 1981.
- Vaupel, P., Manz, R., Mueller-Klieser, W., and Grunewald, W. A. Intracapsillary HbO_2 saturation in malignant tumors during normoxia and hyperoxia. *Microvasc. Res.*, **17**: 181–191, 1979.
- Mueller-Klieser, W., Vaupel, P., Manz, R., and Schmideder, R. Intracapsillary oxyhemoglobin saturation of malignant tumors in humans. *Int. J. Radiat. Oncol. Biol. Phys.*, **7**: 1397–1404, 1981.
- Rofstad, E. K., Fenton, B. M., and Sutherland, R. M. Intracapsillary HbO_2 saturations in murine tumours and human tumour xenografts measured by cryospectrophotometry: relationship to tumour volume, tumour pH and fraction of radiobiologically hypoxic cells. *Br. J. Cancer*, **57**: 494–502, 1988.
- Garewal, H. S., Ahmann, F. R., Schiffman, R. B., and Celniker, A. ATP assay: ability to distinguish cytostatic from cytotoxic anticancer drug effects. *J. Natl. Cancer Inst.*, **77**: 1039–1045, 1986.
- Evanochko, W. T., Ng, T. C., and Glickson, J. D. Application of *in vivo* NMR spectroscopy to cancer. *Magn. Reson. Med.*, **1**: 508–534, 1984.
- Sostman, H. D., Armitage, I. M., and Fisher, J. J. NMR in cancer. I. High resolution spectroscopy of tumors. *Magn. Reson. Imag.*, **2**: 265–278, 1984.
- Beaney, R. P., Lammertsma, A. A., Jones, T., McKenzie, C. G., and Halnan, K. E. Positron emission tomography for *in vivo* measurements of regional blood flow, oxygen utilization, and blood volume in patients with breast carcinoma. *Lancet*, **1**: 131–134, 1984.
- Lammertsma, A. A., Wise, R. J. S., Cox, T. C. S., Thomas, D. G. T., and Jones, T. Measurement of blood flow, oxygen utilization, oxygen extraction ratio, and fractional blood volume in human brain tumours and surrounding oedematous tissue. *Br. J. Radiol.*, **58**: 725–734, 1985.
- Mueller-Klieser, W., Walenta, S., Paschen, W., Kallinowski, F., and Vaupel, P. Metabolic imaging in microregions of tumors and normal tissues with bioluminescence and photon counting. *J. Natl. Cancer Inst.*, **80**: 842–848, 1988.
- Mueller-Klieser, W., Walenta, S., Kallinowski, F., and Vaupel, P. Tumor physiology and cellular microenvironments. *In*: J. D. Chapman, L. J. Peters, and H. R. Withers (eds.), *Prediction of Tumor Treatment Response*, pp.

- 265–276. Elmsford, NY: Pergamon Press, 1988.
16. Thomson, J. E., and Rauth, A. M. An *in vitro* assay to measure the viability of KHT tumor cells not previously exposed to culture conditions. *Radiat. Res.*, *58*: 262–276, 1974.
 17. Twentyman, P. R., Brown, J. M., Gray, J. W., Franko, A. J., Scoles, M. A., and Kallman, R. F. A new mouse tumor model system (RIF-1) for comparison of end-point studies. *J. Natl. Cancer Inst.*, *64*: 595–604, 1980.
 18. Rofstad, E. K., DeMuth, D., Fenton, B. M., and Sutherland, R. M. ³¹P nuclear magnetic resonance spectroscopy studies of tumor energy metabolism and its relationship to intracapillary oxyhemoglobin saturation status and tumor hypoxia. *Cancer Res.*, *48*: 5440–5446, 1988.
 19. Gayeski, T. E. J. A cryogenic microspectrophotometric method for measuring myoglobin saturation in subcellular volumes: Application to resting dog gracilis muscle. Ph.D. Dissertation, University of Rochester, 1981.
 20. Rofstad, E. K., Howell, R. L., DeMuth, P., Ceckler, T. L., Sutherland, R. M. ³¹P NMR spectroscopy *in vivo* of two murine tumor lines with widely different fractions of radiobiologically hypoxic cells. *Int. J. Radiat. Biol.*, *54*: 635–649, 1988.
 21. Vaupel, P., Okunieff, P., Kallinowski, F., and Neuringer, L. J. Correlations between ³¹P-NMR spectroscopy and tissue O₂ tension measurements in a murine fibrosarcoma. *Radiat. Res.*, in press, 1990.